Journal of Biomolecular NMR **28:** 11–29, 2004.
KLUWER/ESCOM

Rotational-echo double-resonance NMR-restrained model of the ternary complex of 5-enolpyruvylshikimate-3-phosphate synthase

Lynda M. McDowell[a,*], Barbara Poliks[b], Daniel R. Studelska[a,**], Robert D. O'Connor[a], Denise D. Beusen[c,***] & Jacob Schaefer[a]
[a]*Department of Chemistry, Washington University, One Brookings Drive, St. Louis, MO 63130, U.S.A.*
[b]*Department of Physics, Binghamton University, Binghamton, NY 13902, U.S.A.*
[c]*Center for Molecular Design, Washington University School of Medicine, St. Louis, MO 63110, U.S.A.*

Received 25 April 2003; Accepted 25 July 2003

Key words: 5-enolpyruvylshikimate-3-phosphate synthase, interatomic distances, molecular modeling, solid-state NMR structure, stable-isotope label

Abstract

The 46-kD enzyme 5-enolpyruvylshikimate-3-phosphate (EPSP) synthase catalyzes the condensation of shikimate-3-phosphate (S3P) and phosphoenolpyruvate to form EPSP. The reaction is inhibited by N-(phosphonomethyl)-glycine (Glp), which, in the presence of S3P, binds to EPSP synthase to form a stable ternary complex. We have used solid-state NMR and molecular modeling to characterize the EPSP synthase–S3P–Glp ternary complex. Modeling began with the crystal coordinates of the unliganded protein, published distance restraints, and information from the chemical modification and mutagenesis literature on EPSP synthase. New inter-ligand and ligand-protein distances were obtained. These measurements utilized the native ^{31}P in S3P and Glp, biosynthetically ^{13}C-labeled S3P, specifically ^{13}C and ^{15}N labeled Glp, and a variety of protein-^{15}N labels. Several models were investigated and tested for accuracy using the results of both new and previously published rotational-echo double resonance (REDOR) NMR experiments. The REDOR model is compared with the recently published X-ray crystal structure of the ternary complex, PDB code 1G6S. There is general agreement between the REDOR model and the crystal structure with respect to the global folding of the two domains of EPSP synthase and the relative positioning of S3P and Glp in the binding pocket. However, some of the REDOR data are in disagreement with predictions based on the coordinates of 1G6S, particularly those of the five arginines lining the binding site. We attribute these discrepancies to substantive differences in sample preparation for REDOR and X-ray crystallography. We applied the REDOR restraints to the 1G6S coordinates and created a REDOR-refined xray structure that agrees with the NMR results.

Abbreviations: CCD – Cambridge Crystallographic Database; CP – cross-polarization; CVFF – consistent valence force field; DTE – dithioerythritol; EPSP 5-enolpyruvylshikimate-3-phosphate; Glp – N-(phosphonomethyl)-glycine; MOPS – 3-[N-Morpholino]propanesulfonic acid; PDB – Protein Data Bank; PEG – poly(ethylene glycol); REDOR – rotational-echo double resonance; RF – radiofrequency; SEDRA – simple excitation for dephasing of rotational-echo amplitudes; SRP – single refocusing-pulse; S3P, shikimate-3-phosphate.

Introduction

Synthesis of aromatic amino acids in plants and microorganisms employs 5-enolpyruvylshikimate-3-phosphate (EPSP) synthase (EC 2.5.1.19) to catalyze the reversible condensation of shikimate-3-phosphate (S3P) and phosphoenolpyruvate (PEP), forming EPSP (Anderson and Johnson, 1990), a substrate for chorismate synthase (Mousedale and Coggins, 1985). This reaction is inhibited by N-(phosphonomethyl)glycine,

*To whom correspondence should be addressed, E-mail: mcdowell@wuchem.wustl.edu
**Current Address: Department of Pathology and Immunology, Washington University School of Medicine, 660 S. Euclid, St. Louis, MO 63110, U.S.A.
***Present address: 1118 Dunston Drive, St. Louis, MO 63146, U.S.A.

$HO_3PCH_2NHCH_2COOH$, (Steinrücken and Amrhein, 1980), which is also known as glyphosate (Glp). It is the active ingredient in the commercial herbicide Roundup® (reviewed in Franz et al., 1997). In the presence of S3P, Glp binds to EPSP synthase and forms a stable, ternary complex (Anderson et al., 1988). Glyphosate is safe in the environment because the shikimate pathway is not present in mammals and because the herbicide is readily inactivated by soil bacteria (Rueppel et al., 1977).

A 3-Å crystal structure of unliganded EPSP synthase was published a decade ago (Stallings et al., 1991), but crystals of the ternary complex suitable for diffraction studies were elusive. Insights into the structure of this complex are fundamentally important to an understanding of the behavior of the enzyme (Studelska et al., 1997). Thus, several years ago, we embarked on what was to become a complete solid-state NMR characterization of the ternary complex, using the unliganded crystal structure as a starting point. Our four part strategy (McDowell et al., 1996a, b) consisted of (1) measuring distances between S3P and Glp (Christensen and Schaefer, 1993; McDowell et al., 1996a), (2) measuring distances from side-chain ^{15}N labels in the basic amino acid residues of EPSP synthase to the S3P phosphate and the carboxyl and phosphonate groups of Glp (McDowell et al., 1996b), (3) using mutagenesis to locate ^{19}F labels in tryptophans in the upper and lower domains of EPSP synthase and then measuring long-range ^{19}F-^{31}P REDOR distances (Studelska et al., 1996) to determine the extent to which the open, unliganded enzyme structure (Stallings et al., 1991) closed around the ^{31}P-containing ligands, and (4) using REDOR-restrained molecular modeling to create a closed, liganded enzyme structure. The previously published distances (McDowell et al., 1996a, b; Studelska et al., 1996) are summarized in Table 1.

Many uncertainties in the preliminary closed enzyme model (Studelska et al., 1996) led to additional measurements (see Results) and a new model, all of which are reported here. Although the xray crystal structure of the ternary complex recently appeared in the literature (Schönbrunn et al., 2001, Protein Data Bank (PDB) (Berman et al., 2000) code 1G6S), most of our modeling and measurements were done before it appeared. Thus, we describe our strategy for assignment and model construction as a general guide for situations where only an unliganded crystal structure exists and solid-state NMR is being used to characterize the liganded structure.

REDOR models were built under the assumption that the structure of the two globular domains would be similar in the open and closed forms of the enzyme. Bond angle adjustments in the 'hinge' region were used to bring the domains closer together and satisfy the long-range restraints (Studelska et al., 1996). Most REDOR restraints were short-range and restricted to the immediate vicinity of the binding site (Christensen and Schaefer, 1993; McDowell et al., 1996a, b). The modeling required an initial assignment of the observed REDOR distances to specific sidechain interactions. This effort relied heavily on the chemical modification and mutagenesis literature for EPSP synthase. Studies conducted with EPSP synthase from *E. coli* and from related plant enzymes that are cited here refer to the *E. coli* amino-acid numbers (Altschul et al., 1990). There are 8 histidine residues in EPSP synthase (Duncan et al., 1984), but only His385 is in the cleft region (Stallings et al., 1991). Photooxidation experiments showed His385 to be at the Glp-binding site (Huynh, 1993), but it is not essential for Glp binding (Shuttleworth et al., 1994, 1996). Of the 17 lysines in EPSP synthase (Duncan et al., 1984), four are in the vicinity of the cleft (Stallings et al., 1991). Of these, Lys22 (Huynh et al., 1988a, b; Huynh, 1990, 1992; Selvapandiyan, 1996), Lys340 (Huynh, 1990), and Lys411 (Huynh, 1991) were identified as being in the active site. About 6 of the 21 arginine residues in EPSP synthase (Kim et al., 1996) are in the cleft region (Stallings et al., 1991). Padgette et al. discovered that arginine-directed phenylglyoxal inactivation could be prevented by the prior formation of the S3P-glyphosate complex. The protected residues were Arg27 and Arg124 (Padgette et al., 1988). The specific association of Arg27 with S3P binding came later (Selvapandiyan, 1996). The R100K mutation resulted in enhanced Glp inhibition, suggesting that Arg100 was specifically associated with Glp binding (Selvapandiyan et al., 1995). This was consistent with observations that the mutations P101S (Stalker et al., 1985) and G96A (Padgette et al., 1991) provided Glp resistance to the enzyme. The above assignments were upheld in later mutagenesis (Shuttleworth et al., 1999) and structural studies (Franz et al., 1997; Krekel et al., 1999; Stauffer et al., 2001a, b). The REDOR $^{31}P\{^{15}N\}$ total dephasing required two more arginine interactions (McDowell et al., 1996b) than those which could be inferred from the literature. We chose Arg344 and Arg386 based on the proximity of Arg344 to Lys340, and Arg386 to His385.

Table 1. Comparisons of internuclear distances used as restraints in molecular dynamics simulations with the corresponding distances in the REDOR model, the crystal structure 1G6S, and the REDOR-refined structure based on 1G6S

Atom pair	Input restraint [Å] [a]	REDOR model [Å]	1G6S [Å]	REDOR refined [Å]
	Intramolecular Glp			
P – C1	5.2–5.5 [b,c]	5.2	5.1	5.2
P – C2	4.2–4.4 [c]	4.1	4.1	4.1
	Inter-ligand S3P – Glp			
P – P	7.6–9.5 [c]	7.5	6.9	7.2
P – C3	7.0–7.3 [c]	7.4	6.4	7.4
P – N	7.1–9.0 [c]	7.2	7.0	7.0
P – C2	6.8–7.1 [c]	7.2	7.1	7.2
P – C1	7.9–8.7 [b,c]	8.3	8.1	8.5
C5 – N	4.2 [d]	4.2	3.6	4.2
	Ligand-residue Glp – Trp			
P – F (172)	11 [e]	11	– [h]	11
P – F (337)	16 [e]	16	16	16
	Ligand-residue S3P – Trp			
P – F (172)	8.5 [e]	8.5	– [h]	8.8
P – F (337)	16 [e]	16	14	15
	Ligand-residue Glp – His			
P – Nδ1 (385)	6.5 – 8.0 [f]	6.4	8.3	9.2
P – Nε2 (385)	6.5 – 8.0 [f]	8.0	6.6	7.2
C1 – Nδ1 (385)	2.9 [d]	3.2	3.7 [i]	3.5 [i]
	Ligand-residue S3P – Arg			
O4 – Nζ1 (27)	3.0 [g]	3.0	2.7	2.7
O5 – Nζ2 (27)	3.0 [g]	3.0	2.8	2.8
	Ligand-residue Glp – Lys			
P – Nε (22)	4.4 [f]	4.4	4.0 [j]	4.3 [j]
P – Nε (411)	4.3 [f]	4.3	4.2 [j]	4.3 [j]
C1 – Nε (411)	4.1 [f]	4.1	4.0 [j]	4.1 [j]
	Ligand-residue S3P – Lys			
P – Nε (340)	3.8 [f]	3.8	3.8	3.7

For completeness, the best-fit REDOR model described in this paper is compared with 1G6S to show that our four-part strategy was largely successful. The comparison validates our assumption that the two globular domains had similar structures in liganded and unliganded forms of the enzyme. It also shows that the solid-state NMR restraints used to create the REDOR model gave protein closure and ligand positions that are similar to the X-ray structure. Thus, efforts to use REDOR restraints to build an accurate model of the *liganded* binding site of a protein should be generally successful even though the only other information available is for the *unliganded* protein. But, there are differences between our REDOR model and 1G6S, particularly with respect to the detailed positioning of the arginine sidechains in the binding site. These are explained by the inherent differences in the state of the protein in the two experiments. The REDOR sample is produced from a frozen solution of the protein complex and is conformationally heterogeneous. The xray sample is a crystal and is conformationally homogeneous. We have discovered that relatively minor changes in 1G6S sidechain positions yielded a REDOR-refined version of the X-ray

Table 1. Continued

Atom pair	Input restraint [Å] [a]	REDOR model [Å]	1G6S [Å]	REDOR refined [Å]
	Ligand-residue Glp – Arg			
P – Nζ1 (124)	3.6 [d,k]	3.6	3.5	3.8 (3.8) [k,l]
P – Nζ2 (124)	3.6 [d,k]	3.6	3.8	3.8 (3.8) [k,l]
P – Nε (124)	5.6 [d,m]	5.4	5.4	5.6 (5.6) [l,m]
P – Nζ1 (100)	4.0 [d,k]	4.0	6.9	3.9 (3.9) [k,l]
P – Nζ2 (100)	4.0 [d,k]	4.0	5.3	3.5 (3.4) [k,l]
P – Nε (100)	5.7 [d,m]	5.8	7.0	5.5 (5.5) [l,m]
C1 – Nζ1 (344)	3.4 [d,k]	3.4	3.6	5.5 (5.5) [k,l,n]
C1 – Nζ2 (344)	5.6 [d,k]	5.5	3.6	3.4 (3.3) [k,l,n]
C1 – Nε (344)	4.5 [d,o]	4.4	5.3	4.9 (4.8) [k,l,o]
C1 – Nζ1 (386)	2.8 [d,k]	3.0	3.8	4.9 (4.9) [k,l,
C1 – Nζ2 (386)	4.9 [d,k]	4.8	5.4	3.0 (2.7) [k,l]
C1 – Nε (386)	4.8 [d,o]	4.8	3.4	4.3 (4.4) [k,l,o]

[a] A 10% range in the pair distance is assumed unless noted otherwise.
[b] From Christensen and Schaefer (1993). The C-3 of Glp is directly bonded to N and P; the C-1 is the terminal carboxyl carbon. This numbering scheme was used in McDowell et al. (1996a, b) and is continued in this work. The PDB reverses the C-1 and C-3 assignments and refers to Glp as "GPJ."
[c] From McDowell et al. (1996a).
[d] This work.
[e] From Studelska et al. (1996).
[f] From McDowell et al. (1996b).
[g] From Franz et al. (1997) and the REDOR results of Figure 4.
[h] 1G6S has Phe172 and not Trp172.
[i] The distance to Nε2 (385) is also too large to match the REDOR data.
[j] The assignments of Lys22 and Lys411 are reversed in 1G6S.
[k] Assignment of restraints was model dependent (see the description of modeling in text). The error in distances is estimated as ± 0.2 Å, based on the distance changes needed to give noticeably poorer fits to the data in Figure 9.
[l] The restraints used for the refinement of 1G6S are shown in parentheses.
[m] Assignment of restraints was model dependent. The allowed values from Figure 5 are 4.5–5.7 Å.
[n] The assignments of Nζ1 and Nζ2 distances are reversed in the REDOR-refined structure. Dephasing due to Nζ1 is indistinguishable from dephasing due to Nζ2; thus both assignments are consistent with the REDOR results.
[o] Assignment of restraints was model dependent. There was no NMR measurement of these distances.

structure that agrees better with the NMR data than does 1G6S.

Materials and methods

Ring-labeled ^{13}C shikimate-3-phosphate

Glucose with singly ^{13}C-enriched carbons was used to biosynthetically label carbons in the shikimate ring of S3P. The method involved a *Klebsiella pneumoniae* strain (A170-40, purchased from the American Type Culture Collection as ATCC#25597) that released S3P into the medium. This is the cell line that allowed Weiss and Mingioli (1956) to characterize S3P as an essential precursor for aromatic amino acid synthesis. We employed their method of S3P production and purification, described in protocol form by Knowles and Sprinson (1970). S3P levels were assayed by the determination of shikimic acid (Millican, 1970) after enzymatic hydrolysis with potato acid phosphatase (Knowles and Sprinson, 1970). S3P-enriched supernatants were harvested from cells grown overnight in a defined medium containing either D-[5-^{13}C]glucose or D-[3-^{13}C]glucose (99% enrichment, Cambridge Isotope Laboratories, Andover, MA). D-[5-^{13}C]glucose was supplied at 5 mg/ml, whereas D-[3-^{13}C]glucose was at 2.5 mg/ml, supplemented with 2.5 mg/ml sodium pyruvate and 25 μg/ml agaric acid. The latter supplements enhanced S3P yield in pilot experiments. The medium also contained 7 mg/ml K_2HPO_4, 3 mg/ml KH_2PO_4, 0.1 mg/ml $MgSO_4 \cdot 7H_2O$, 1 mg/ml $(NH_4)_2SO_4$, 0.3 mg/ml NaCl, 10 μg/ml L-tyrosine, 10 μg/ml L-phenylalanine, 5 μg/ml L-tryptophan,

10 ng/ml p-aminobenzoic acid, and 10 ng/ml p-hydroxybenzoic acid. Isotopic enrichment was assayed by solution-state proton NMR of the barium or potassium salt of purified S3P. The [5-^{13}C] glucose yielded [1, 3-$^{13}C_2$] S3P, with 68% incorporation at C1 and 80% incorporation at C3. The [3-^{13}C] glucose yielded [4, 5, 7-$^{13}C_3$] S3P, with 11% incorporation at C4, 63% incorporation at C5, and 30% at C7.

Expression, purification and complex formation of ^{15}N-arginine labeled enzyme from an E. coli auxotroph

Wild-type *E. coli* EPSP synthase was overexpressed in an *E. coli* strain auxotrophic for arginine (ATTC #23790) to increase the incorporation of L-[ζ-$^{15}N_2$]arginine (99% enrichment, Cambridge Isotope Laboratories, Andover, MA) into the enzyme. The expression system was made by transformation of ATTC #23790 with pMON5537 (Olins et al., 1988). The transformed cells were stored as frozen glycerol stocks. A colony of these cells was selected from a 37 °C, 18-h agar plate made with Luria–Bertani media containing ampicillin at 200 μg/ml (LB/AMP). The colony was transferred to 6 ml of liquid LB/AMP and incubated overnight in an orbital shaking incubator at 225 rpm and 37 °C. These cells were used to inoculate two 250 ml flasks each containing 50 ml of unlabeled defined growth medium. The unlabeled defined medium contained: 12.8 mg/ml $Na_2HPO_4{\cdot}7H_2O$, 3 mg/ml KH_2PO_4, 0.5 mg/ml NaCl, 77.8 μg/ml thiamine-HCl, 6 μg/ml $FeCl_3$, 100 μg/ml ampicillin, 4 mg/ml D-glucose, 1 mg/ml NH_4Cl, 0.44 μg/ml ZnSO4·7H_2O, 0.78 μg/ml $Na_2MoO_4{\cdot}2H_2O$, 0.892 μg/ml $CuSO_4{\cdot}5H_2O$, 0.22 μg/ml H_3BO_3, 0.56 μg/ml $MnSO_4{\cdot}H_2O$, 0.78 μg/ml $CoCl_2{\cdot}6H_2O$, 2mM $MgSO_4$, 100 μM $CaCl_2$, 225 μg/ml L-alanine, 37.5 μg/ml L-arginine, 100 μg/ml L-asparagine, 125 μg/ml L-aspartate, 37.5 μg/ml L-cysteine, 100 μg/ml L-glutamic acid, 100 μg/ml L-glutamine, 250 μg/ml glycine, 37.5 μg/ml L-histidine, 125 μg/ml L-isoleucine, 250 μg/ml L-leucine, 100 μg/ml L-lysine, 75 μg/ml L-methionine, 75 μg/ml L-phenylalanine, 100 μg/ml L-proline, 125 μg/ml L-serine, 160 μg/ml L-threonine, 16 μg/ml L-tryptophan, 75 μg/ml L-tyrosine, and 160 μg/ml L-valine. At mid log phase (OD_{600} = 1.2), ten ml aliquots of this growth were used to inoculate ten 1000 ml flasks each containing 400 ml of the same defined medium. The bacteria from the 1000 ml flasks were pelleted at mid-log phase. Each pellet was resuspended in 400 ml of a labeled defined medium that was similar to the unlabeled medium except that it contained 115 μg/ml L-[guanidino-$^{15}N_2$]arginine instead of unlabeled L-arginine, 50 μg/ml L-cysteine, and 50 μg/ml L-histidine. The resuspended cells, returned to 1000 ml flasks, were incubated, as before, 30 min (to OD_{600} = 1.6) before EPSP synthase overexpression was induced by addition of nalidixic acid at 75 μg/ml. Incubation continued for 9.5 h before the cells were pelleted and frozen. Protein purification was as described previously (Christensen and Schaefer, 1993; McDowell et al., 1996b). The yield of purified enzyme was 105 mg/l of labeled medium. Isotopic enrichment was determined by solid-state ^{15}N NMR spin counts (McDowell et al., 1996b) as 82%.

A 120 mg aliquot of [ζ-$^{15}N_2$]Arg-EPSP synthase was incubated 1:1:1 with glyphosate and the potassium salt of [1, 3-^{13}C]S3P at 87 μM in 30 ml of ice-cold buffer for 35 min in a 300 ml lyophilization flask. The buffer contained: 0.2% (w/v) PEG 8000, 25 mM trehalose, 1 mM DTE and 2mM MOPS/KOH, pH 7.45. The sample was slowly frozen to −20 °C, cooled to −70 °C, and then placed in liquid nitrogen during attachment to a lyophilizer.

Expression, purification, and complex formation of enzyme from W3110/pMON5537

Natural abundance EPSP synthase and [^{15}N]Gly-EPSP synthase were expressed, purified, and complexed essentially as described previously (Christensen and Schaefer, 1993; McDowell et al., 1996b), except twice the usual amount of [^{15}N]Gly (200 mg/l; Merck Stable Isotopes, 95% isotopic enrichment) was added to the growth media. The [^{15}N]Gly growth media also contained 200 mg/l L-[1-^{13}C]Ala (Merck Stable Isotopes, 90% isotopic enrichment), but that label was not needed for the experiments reported here. Unlabeled S3P and Glp were complexed with 160 mg [^{15}N]Gly-EPSP synthase.

Two 180 mg aliquots of unlabeled enzyme were each incubated 1:1:1 with the potassium salt of [4, 5, 7-$^{13}C_3$]S3P and either natural abundance glyphosate or [3-^{13}C, ^{15}N]Glp in an ice-cold buffer containing 1 mM DTE and 2 mM MOPS/KOH, pH 7.2. (Glp C-3 is directly bonded to N and P; Glp C-1 is the terminal carboxyl carbon. This is the numbering scheme used in our previous publications (Christensen and Schaefer, 1993; McDowell et al., 1996a, b). The PDB numbering scheme reverses the C-1 and C-3 assign-

ments and refers to Glp as 'GPJ.') All components of these two preparations were at 43.6 μM in 80 ml final volume in 300 ml lyophilization flasks. After 25 min. the samples were shell-frozen and attached to a lyophilizer. After vacuum seals were obtained, lyophilization flasks were at room temperature for ensuing primary and secondary drying.

REDOR

Rotational-echo, double-resonance (REDOR) NMR provides a direct measure of heteronuclear dipolar coupling between isolated pairs of labeled nuclei in solids spinning at the magic angle (Gullion and Schaefer, 1989a, b). The S-spin (observed) rotational echoes that form each rotor period following a proton to S-spin cross-polarization (CP) transfer can be prevented from reaching full intensity by insertion of I-spin (dephasing) π pulses. (The shorthand observed{dephasing} is used to specify the nuclei in these REDOR experiments.) The REDOR difference ($\Delta S = S_0 - S$) is the difference between an S-spin NMR spectrum obtained with no I-spin dephasing π pulses (S_0), and one obtained under dephasing conditions (S). The $\Delta S/S_0$ ratio has a strong dependence on the dipolar coupling and hence the internuclear distance (Gullion and Schaefer, 1989a).

All REDOR experiments have two π pulses per rotor period, but these pulses can be distributed between the I and S channels in a variety of ways (Gullion and Schaefer, 1989b). At least one S-spin π pulse in the center of the evolution period is required to refocus isotropic chemical shifts (Gullion and Schaefer, 1989b). Unless there are multiple, homonuclear coupled S-spins, the optimal REDOR experiment for biological samples has I-spin π pulses at the half-rotor cycles, and S-spin π pulses at each integral rotor cycle (Hing et al., 1994; McDowell et al., 1996b). Both sets of π pulses are applied using the xy8 phase-cycling scheme (Gullion et al., 1990; Gullion and Schaefer, 1991) to suppress offset effects and compensate for pulse imperfections. An additional S-spin π pulse and two rotor periods without REDOR evolution are added at either the center (Hing et al., 1994) or the end (McDowell et al., 1996b) of the dipolar evolution to permit data acquisition without pulse interference. This interleaved REDOR scheme was used for the squares and 'x's of Figure 1, and for all EPSP synthase data for which a different sequence is not explicitly described below.

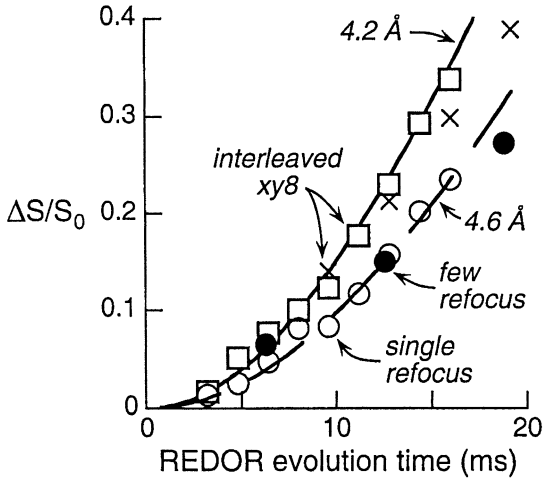

Figure 1. Accuracy of REDOR pulse sequences. The [1-^{13}C]MeA2-[^{15}N]Gly6 distance in the benzyl ester of emerimicin 1-9 (a helical peptide) was 4.16 Å by xray analysis (Marshall et al., 1990). Interleaved xy8 REDOR (squares, 2400 scans; and 'x's, 2048 scans, with 5 kHz MAS) gave the most accurate results. SRP REDOR results (open circles, 2400 scans, 5 kHz MAS) were always accurate to within 10%, but evolution times $\leqslant 8$ ms had better accuracy (within 5%). REDOR with 8-refocusing pulses (solid circles, 2048 scans, 5102 Hz MAS) gave better sensitivity than SRP REDOR for some carbons, and had acceptable accuracy.

REDOR in the presence of homonuclear coupling

The strong homonuclear ^{13}C-^{13}C couplings in [1, 3-$^{13}C_2$]S3P and [4, 5, 7-$^{13}C_3$]S3P could cause spectral artifacts due to the SEDRA effect (Gullion and Vega, 1992) if the interleaved REDOR sequence were used. For the [1, 3-$^{13}C_2$]S3P complex (see Results), a single refocusing pulse (SRP) on ^{13}C was utilized (Beusen et al, 1995). Normally, we use "short evolution times" to describe the range of conditions under which theory and experiment agree in the SRP REDOR experiment. In our hands, this pulse sequence provided accurate results for evolution times $\leqslant 8$ ms on our 200-MHz spectrometers (Pan et al., 1990; Marshall et al., 1990; Mehta et al., 2000; Wu et al., 2000). We have repeated the published experiments on [1,3-$^{13}C_2$, ^{15}N]Ala (Mehta et al., 2000) on our 300-MHz spectrometer and obtained similar results (not shown). However, Chan and Eckert (2000) have reported deviations (less dephasing than expected theoretically) due to experimental imperfections at what we normally consider short evolution times. The magnitude of these deviations probably depends on the spectrometer, the probe, and the spin characteristics of the sample (Chan and Eckert, 2000; Weldeghiorghis and Schaefer, 2003). This implies that the accurate range

of evolution times will differ from one laboratory to another, and between various experimental conditions within the same laboratory.

SRP REDOR is less accurate than interleaved xy8 when the evolution time is long ($\geqslant 10$ ms, see below). Measurement of the weak heteronuclear dipolar couplings in most biological samples requires long REDOR evolution times (see Figure captions). SRP REDOR also had low sensitivity when used for the EPSP synthase-[4, 5, 7-$^{13}C_3$]S3P-Glp ternary complex, particularly for the carboxyl label (not shown). Better sensitivity (see Results) was obtained by using 8 refocusing pulses distributed over the REDOR evolution period (O'Connor and Schaefer, 2002). We added a two-rotor cycle Hahn echo between the CP transfer and REDOR evolution for these experiments. The same sample used to validate weak-coupling determinations at 200 MHz (Marshall et al., 1990; Hing et al., 1994) was used to compare the three pulse sequences on our 300 MHz spectrometer (Figure 1). The interleaved xy8 REDOR (Figure 1, squares) was accurate over a large range of evolution times, although repeating the experiment after 8 years (Figure 1, 'x's) showed some variability at the longest evolution times. For evolution times up to 8 ms, SRP REDOR results (Figure 1, open circles) were the same as, or within 5% of, interleaved xy8 REDOR results (Figure 1, squares and 'x's). At 10 ms and beyond, the SRP REDOR determined distance was 10% larger than the theoretical value. The 8-refocusing pulse REDOR results (Figure 1, solid circles) spanned the range of the two more established experiments. Its greatest strength was increased sensitivity (improved refocusing for S_0), particularly for off-resonance peaks with large chemical shift anisotropy.

Double REDOR

Double REDOR consists of two separate REDOR experiments performed sequentially (Beusen et al., 1995). The first REDOR sequence is designed to remove interferences from the natural-abundance ^{13}C background. For example, if the ^{13}C labels are introduced with a ^{31}P nearby, then the $^{13}C\{^{31}P\}$ ΔS arises exclusively from the ^{13}C labels. This spectrum becomes the reference for a measurement of the coupling to a third label, typically ^{15}N or ^{19}F. Double REDOR spectra of EPSP synthase-[4, 5, 7-$^{13}C_3$]S3P-[3-^{13}C, ^{15}N]Glp involved the use of relatively strong ^{31}P-^{13}C dipolar coupling within the labeled S3P to obtain a natural-abundance ^{13}C background-free spectrum. The $^{13}C\{^{15}N\}$ part of the double REDOR experiment then measured ^{13}C-^{15}N dipolar coupling between labels in S3P and Glp.

When both sets of REDOR experiments in double REDOR are performed back-to-back within the same pulse sequence, then the effects of temperature variations on amplifier performance and probe tuning are all taken into account automatically by active control of the radiofrequency (RF) levels of all channels. Because fewer scans were needed for the large $^{13}C\{^{31}P\}$ ΔS than for the small $^{13}C\{^{15}N\}$ ΔS (see Results), experiment time was reduced by performing the two sets of REDOR experiments separately. Scaling was done by comparison of the S_0 spectra in each of the REDOR experiments. The pulse sequences generating these spectra were identical.

Solid-state NMR spectrometer

Spectra were obtained on powder samples using a 7.05-T Oxford magnet, a three-channel Chemagnetics console (Fort Collins, CO) modified to time-share a fourth channel and include feedback control of RF power levels, and a four-channel ^{1}H, ^{31}P, ^{13}C, and ^{15}N transmission-line probe (at 300, 121, 75, and 30 MHz, respectively), all of which have been described previously (McDowell et al., 1996a, b). CP transfers were performed for 1 or 2 ms at 50 kHz. The sequence-repetition time was 2 s. Refocusing and dephasing π pulses were 10 μs. The continuous wave proton decoupling RF field intensity was 90 kHz. Experiments were done at room temperature, unless noted otherwise. The magic-angle spinning (MAS) module and 7.5-mm zirconia rotors were obtained from Chemagnetics (Fort Collins, CO, now a division of Varian). A controlled spinning speed of 5000 Hz was used unless noted otherwise. Samples containing multiple ^{13}C labels required different spinning speeds to avoid rotational resonance conditions (Raleigh et al., 1988).

Arginine templates

Figure 2 (solid circles) shows the Glp $^{31}P\{^{15}N\}$ $\Delta S/S_0$ for [ζ-$^{15}N_2$]Arg-EPSP synthase-S3P-Glp as a function of dipolar evolution time. These are the same data shown in Figure 9 (left panel). The solid, dotted, and dashed lines are the calculated REDOR dephasing (McDowell et al., 1996a; Goetz and Schaefer, 1997) for different geometries ('templates') of the multi-spin dephasing system consisting of four ζ-^{15}N labels in two arginine sidechains. Except for the curve

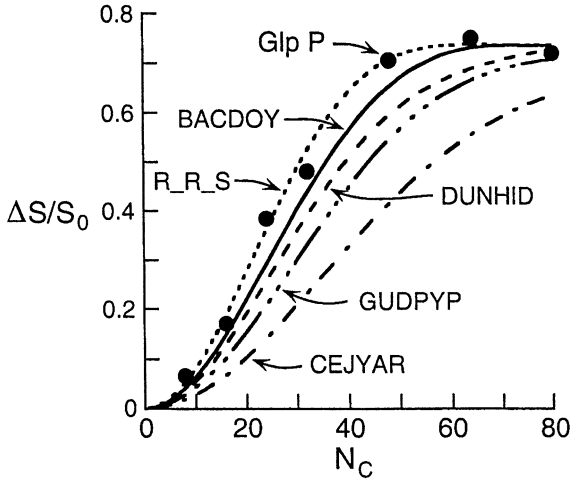

Figure 2. Experimental Glp $^{31}P\{^{15}N\}$ REDOR dephasing ($\Delta S/S_0$) for [ζ-$^{15}N_2$]Arg-EPSP synthase-S3P-[1-^{13}C]Glp (symbols) compared with calculated multi-spin REDOR dephasing (solid, dotted, and dashed lines) for different geometries of four arginine ζ-^{15}N's. Except for the dephasing curve labeled RRS, the labels on the figure correspond to CCD reference codes (see Methods – Arginine templates). The REDOR curves for BACDIS and GUAPST (not shown) are between those of BACDOY and DUNHID. ARGEPO10 (not shown) has a dephasing curve similar to that of GUDPYP. Using the correct number of arginines (21), we re-calculated the arginine ^{15}N isotopic enrichment as 51% and used that value for the dephasing calculations (instead of the 54% enrichment reported in McDowell et al., 1996b, where Figure 11 shows spectra of the 64 rotor cycle data.). This change had a small effect, reducing the dephasing plateau for the BACDOY $\Delta S/S_0$, for example, by 0.03. The MAS speed was 5 kHz. The same sample was used for all experiments. These data are also used in Figure 9 of this work (see Results).

labeled RRS, the geometries are small-molecule mimics of guanidino-like interactions with phosphates or phosphonates from the Cambridge Crystallographic Database (CCD, Cambridge Crystallographic Data Center, 12 Union Road, Cambridge, CB2 1EZ, UK, http://www.ccdc.cam.ac.uk/). The labels correspond to Reference Codes from the CCD. Most of the geometries result in poor fits to the data and can be discarded. To calculate the RRS dephasing curve, the crystallographic sulfate near Arg100 and Arg124 of unliganded EPSP synthase (Stallings et al., 1991) was assumed to be a phosphate. Because RRS seemed the best fit to the data (Figure 2), this geometry was previously used to model the Glp-phosphonate interaction with Arg344 and Arg386 (Studelska et al., 1996). However, the RRS ε-^{15}N to Glp ^{31}P distance of 3.8 Å was much shorter than the measured 4.5–5.7 Å (Figure 2). Thus, we changed to the BACDOY geometry (that has an ε-^{15}N to Glp ^{31}P distance of 5.6 Å) for Glp phosphonate interactions with Arg100 and Arg124. The BACDOY ^{31}P-ζ-^{15}N distances of 3.9, 3.9, 3.8, and 3.8 Å were adjusted during modeling (see below) to improve the agreement with the REDOR data (Figure 2). Even though the model restrained only distances and not a particular hydrogen-bonding pattern, both BACDOY and the REDOR model each have four hydrogen bonds involving guanidino protons.

We also needed to choose a geometry for Arg344 and Arg386 interacting with the Glp carboxyl group. A search of the PDB yielded nine types of 1:1 Arg:carboxyl-group interactions. Modeling was used to build 2:1 Arg:carboxyl-group templates from various combinations of the nine 1:1 interactions. The best fit to the NMR data was obtained by modifying RRS to accommodate a planar carboxyl group instead of a tetrahedral sulfate. The resulting RRC template had ^{13}C to ζ-^{15}N distances of 3.4 and 5.6 Å to one arginine, and 2.8 and 4.9 Å to a second arginine (Table 1) and fit the $^{13}C\{^{15}N\}$ REDOR dephasing for [ζ-$^{15}N_2$]Arg-EPSP synthase-S3P-[1-^{13}C]Glp.

Our EPSP synthase sequence matches the one reported by Kim et al. (1996) and the 1G6S xray structure (Schönbrunn et al., 2001) both of which have Thr330 and Ser23. The structure by Stallings et al. (1991) has Arg330 and Thr23 instead, matching an earlier sequence report (Duncan et al., 1984). We did not change Arg330 and Thr23 to Thr330 and Ser23 for our modeling, but noted the correct number of arginine residues (21) for template calculations.

Molecular modeling

The open x-ray structure of unliganded EPSP synthase (with Phe172 replaced by Trp172, F172W) was the starting structure for building a model of the EPSP synthase-S3P-Glp ternary complex. The coordinates of the open enzyme were obtained from Monsanto. Proton coordinates were added according to the positions of the heavy atoms using Insight II software (Accelrys, Inc., San Diego, CA). S3P (in the chair conformation, Castellino et al., 1991; Leo et al., 1992; Franz et al., 1997; Krekel et al., 1999) and Glp (in the extended conformation) were placed together to satisfy approximately the intra- and inter-ligand REDOR distances (McDowell et al., 1996a). The ligands were put into F172W with the S3P carboxyl group close to Arg27 (Table 1). The enzyme was closed around the ligands by manually adjusting the torsion angles of the P19-G20 and Q240-G241 'hinges' until the distances between the phosphorus on both ligands and the 6-^{19}F labels of Trp172 and Trp337 were in the range

consistent with REDOR measurements (Table 1). (The coordinates of the fluorines were taken as those of the corresponding Trp ring protons.) The Glp orientation was adjusted during the closing process to force its carboxyl group towards His385, Arg344, and Arg386.

Following this closure, a sequence of energy minimizing and dynamics steps was applied (using CVFF forcefields and algorithms from Accelrys, Inc.) with the distances between labeled nuclei of the ligands and selected residues of the enzyme restrained to the ranges measured by REDOR. At first only the restraints on the distances between the phosphorus of S3P and all the heavy atoms of Glp (McDowell et al., 1996a) were added to the ones mentioned above, and the structure was minimized so that the maximum derivative of all energy terms for all atoms was less than 1 kcal $mol^{-1}Å^{-1}$. Following this procedure, protons were added to obtain a pH value of 7.5; Glp and S3P were assigned charges of -2 and -3, respectively. The whole complex was then solvated in a 5-Å layer of water and energy-minimized again with additional restraints on the distances: P(Glp)-^{15}N(Lys22) and P(S3P)-^{15}N(Lys340).

Next, the torsion angles of bonds connecting Lys411 to the backbone were manually adjusted to bring the sidechain ^{15}N close to Glp. Following this adjustment the structure was energy-minimized again, with additional restraints for the distances between ^{31}P(Glp) and ^{15}N(Lys411), and also between the two ends of Glp and Arg100, Arg124, Arg386, and Arg344. The arginines were oriented to satisfy, approximately, the BACDOY and RRC templates described in the previous section. A 20-ps dynamics simulation at 300 K assuming a constant-temperature, constant-volume ensemble with all the restraints listed above maintained at 20 kcal $mol^{-1}Å^{-2}$ followed the energy minimization. Several more minimization-dynamics steps were performed with slight restraint modifications until all of the REDOR data could be described using the coordinates of the resulting structure (REDOR model) and until the derivative of the total energy was 0.1 kcal mol^{-1} $Å^{-1}$. In the early stages of the modeling, REDOR restraints corresponding to 20 kcal mol^{-1} $Å^{-2}$ were used; these were increased to 100 kcal mol^{-1} $Å^{-2}$ in the later stages of modeling.

The coordinates of the final model satisfying the REDOR restraints were evaluated by the ADIT software system used by the PDB for editing and checking data entries. The evaluation report indicated that (i) more than 25% of main-chain C_α-C bond lengths differed by more than 0.05 Å from the small-molecule values; (ii) six of the mainchain bond angles differed by more than 10° from accepted values; and (iii) the planarity of some residues was distorted. To correct these problems, another energy minimization was performed with CVFF bond, angle, and out-of-plane force constants increased to ensure that covalent bonds and residue planarities met the required values. In addition, main-chain torsion angles for 10 residues with the largest deviations from standard Ramachandran values were individually corrected. Before deposition into the PDB, the dephasing calculations were repeated to confirm that the resulting REDOR curves were still a good fit to the experimental data.

Results

S3P-Glp orientation

About 500 relative orientations for S3P-Glp were consistent with our previously reported inter-ligand REDOR results (McDowell et al., 1996a). The lack of specificity arose from the fact that only the ^{31}P of S3P was used in generating inter-ligand restraints to the multiple labels in Glp. Clearly, a second label in S3P would have been useful.

Unlabeled EPSP synthase and [4, 5, 7-$^{13}C_3$]S3P were used to form ternary complexes with either [3-^{13}C,^{15}N]Glp or unlabeled Glp. The large natural-abundance ^{13}C signals from these complexes made using the ^{13}C{^{15}N} full echo spectra (Figure 3, bottom, left and right) impossible for quantification. Instead, the ^{13}C{^{31}P} REDOR differences (Figure 3, center, left and right) were the effective full echoes for distance determinations in a double REDOR experiment (see Methods). The S3P 5-^{13}C signal at 68 ppm had a measured (^{13}C{^{15}N} ΔS) / (^{13}C{^{31}P} ΔS) of 0.35 (Figure 3, left). No correction was needed for dephasing by natural-abundance ^{15}N (Figure 3, right). Based on this dephasing, the measured [5-^{13}C]S3P to [^{15}N]Glp C-N distance is 4.1 Å. Although data from shorter evolution times is often more reliable, a 96 rotor-cycle REDOR experiment gave nearly the same result (4.2 Å, data not shown).

The proximity of the Glp nitrogen to the C-5 of S3P is consistent with the proposed hydrogen-bonding interaction between the amino group of Glp and a hydroxyl of S3P (Anderson and Johnson, 1990). This arrangement is satisfied by only 16 of the 500 REDOR-allowed conformers (McDowell et al., 1996a). All 16 conformers have an S3P O5-Glp N distance less than

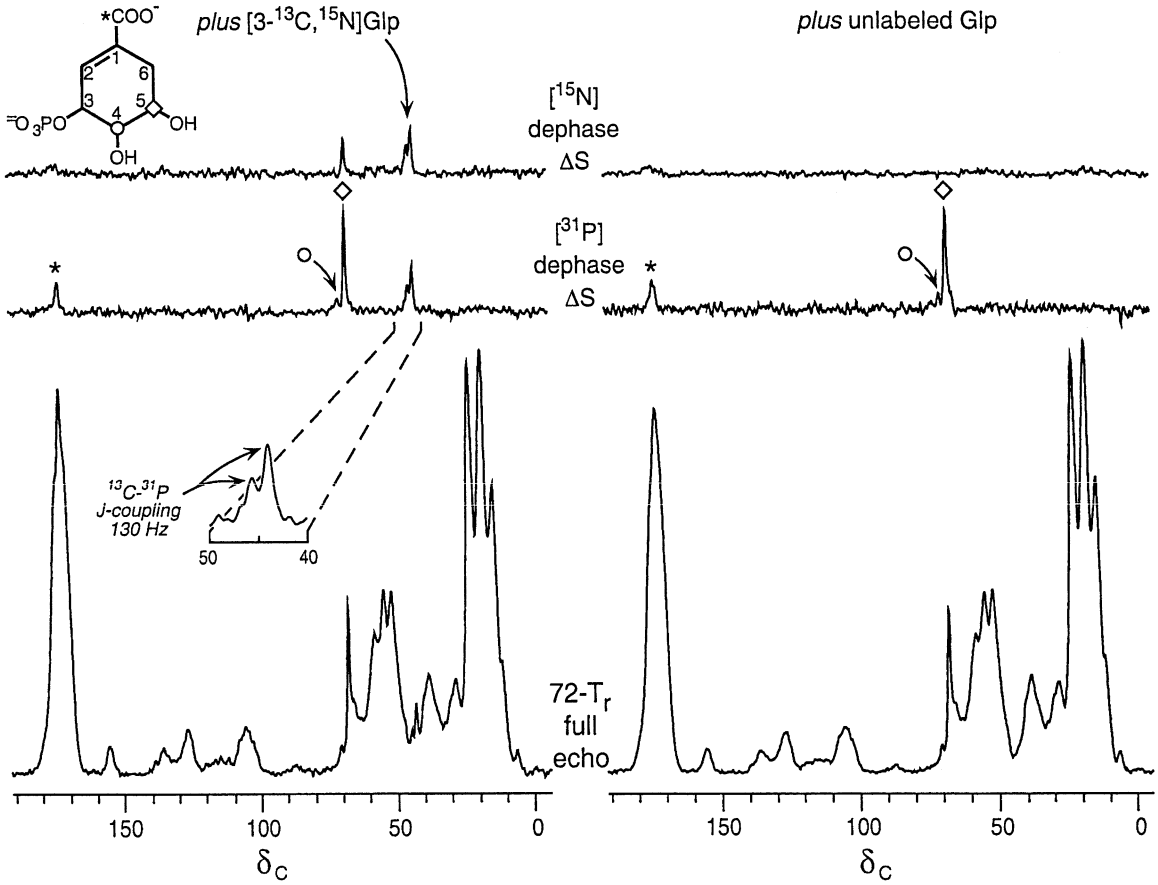

Figure 3. Double REDOR spectra of EPSP synthase-[4, 5, 7-$^{13}C_3$]S3P-[3-^{13}C, ^{15}N]Glp (left) and EPSP synthase-[4, 5, 7-$^{13}C_3$]S3P-Glp (right) lyophilized ternary complexes. The C4 carbon (open circle) had an isotopic enrichment of 11%, the C5 carbon (open diamond), 63%, and the C7 carbon (star), 30%. For the spectra on the left, 36,864 scans were acquired for the $^{13}C\{^{15}N\}$ REDOR difference and full echo (top and bottom, respectively), as well as the $^{13}C\{^{31}P\}$ REDOR difference (center). For the spectra on the right, 102,400 scans were acquired for the $^{13}C\{^{15}N\}$ REDOR difference and full echo (top and bottom, respectively), and 22,528 scans for the $^{13}C\{^{31}P\}$ REDOR difference (center). All spectra have been scaled vertically to account for the total number of scans. Eight ^{13}C-refocusing pulses were used during the 72-rotor cycle (14.1 ms) REDOR evolution period (see Methods). The MAS speed was 5102 Hz.

3.2 Å. No conformer has an S3P O4-Glp N distance in this range (McDowell et al., 1996a).

Proximity of S3P carboxyl group to an arginine sidechain

Evidence for an interaction between an arginine sidechain and the S3P carboxyl group was sought by preparing a ternary complex of [1, 3-$^{13}C_2$]S3P, unlabeled glyphosate, and [ζ-$^{15}N_2$]Arg-EPSP synthase. A $^{13}C\{^{31}P\}$ REDOR difference (Figure 4, top) identifies the [1, 3-$^{13}C_2$]S3P resonances amongst the natural-abundance ^{13}C signals from the protein and buffer that dominate the full-echo spectrum (Figure 4, bottom). Because S3P ^{31}P is at least 5 Å away from its nearest arginine (McDowell et al., 1996b), the 3-^{13}C of S3P is likely to be even farther away. Thus, a $^{13}C\{^{15}N\}$ REDOR difference (ΔS) for the 67-ppm resonance (open square) was neither expected nor observed (Figure 4, center). On the other hand, the 1-^{13}C label could be close to an ^{15}N if an arginine sidechain were interacting with the S3P carboxyl group. This proximity was observed. The 133-ppm [1-^{13}C]S3P resonance and its spinning sidebands (solid circles) are in regions relatively free from natural-abundance signals. Thus, area and peak-height measurements of the full-echo spectrum (S_0, Figure 4, bottom) and ΔS spectrum (Figure 4, center) were averaged to obtain $\Delta S/S_0 = 0.20$. (The true value of $\Delta S/S_0$ could be as high as 0.30; see Methods). For this three-spin system (the 1-^{13}C observed spin and the two ζ-^{15}N dephas-

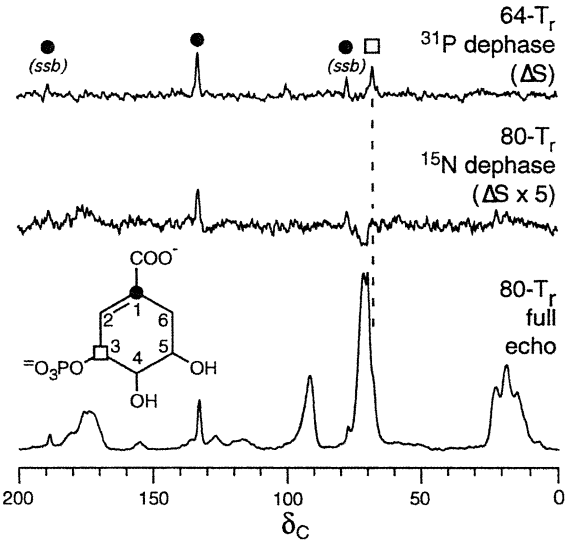

Figure 4. $^{13}C\{^{15}N\}$ REDOR spectra of [ζ-$^{15}N_2$]Arg-EPSP synthase-[1, 3-$^{13}C_2$]S3P-Glp lyophilized ternary complex. The C1 carbon (open square) had an isotopic enrichment of 80%, and the C3 carbon, 68%. The full echo-spectrum is shown at the bottom of the figure and the REDOR difference is in the middle. The spectra (250,144 scans) were taken after 80 rotor cycles (19.2 ms) of REDOR evolution. Area measurements were obtained by spectral deconvolution. Neighboring natural-abundance ^{13}C intensities were subtracted from peak heights of the labeled carbons. The $^{13}C\{^{31}P\}$ REDOR difference spectrum (16,384 scans) shown at the top was taken with 64 rotor cycles, or 15.36 ms, of REDOR evolution. It was scaled vertically to compensate for fewer scans and used only to identify the location of the [3-^{13}C]S3P peak. For all spectra, the MAS speed was 4167 Hz and a single ^{13}C refocusing pulse was used in the center of the REDOR evolution period.

ing spins), geometry and distance are both variables in interpreting the REDOR results (McDowell et al., 1996a; Goetz and Schaefer, 1997). The data can be matched by two arrangements: either the two ^{15}N labels are equidistant from ^{13}C ($\sim$ 4.7 Å), or one ^{15}N is closer (4.3–5.0 Å) and the other farther away (5–7 Å). In either situation, however, the data support a hydrogen-bonding interaction between the ζ-nitrogens of an arginine sidechain and the carboxyl group of S3P.

Proximity of Glp to a histidine sidechain

The $^{13}C\{^{15}N\}$ REDOR full-echo spectrum of [indole-$^{15}N_2$]His-EPSP synthase-S3P-[1-^{13}C]Glp is dominated by the natural-abundance ^{13}C protein carbonyl-carbon peak centered near 175 ppm (not shown). The natural-abundance signal arises from protein carboxyl carbons close to any of the eight $^{15}N_2$-labeled histidines in EPSP synthase. The natural-abundance signals were removed from both full-echo and difference spectra by subtracting the REDOR spectra of an unlabeled ternary complex (not shown; see McDowell et al., 1996b). The resulting observed $^{13}C\{^{15}N\}$ $\Delta S/S_0$ of 0.9 $\pm$ 0.2 for the [1-^{13}C]Glp label places at least one of the indole-^{15}N of His385 (the only histidine in the vicinity of the binding site) well within 4 Å of the label in Glp (Table 1).

Because the $^{31}P\{^{15}N\}$ REDOR difference is only about 0.07 $\pm$ 0.01 for the [indole-$^{15}N_2$]His-EPSP synthase-S3P-[1-^{13}C]Glp (McDowell et al., 1996b), the ^{31}P of Glp is between 6.5 and 8.0 Å from the indole-^{15}N of His385 (Table 1). This means that the carboxyl group of Glp is much closer to His385 than the phosphate group. The ^{31}P Glp to His385 distance determination (McDowell et al., 1996b) assumed that no significant fraction of the Glp $^{31}P\{^{15}N\}$difference was due to natural abundance ^{15}N. This assumption was validated by measuring the Glp $^{31}P\{^{15}N\}$ $\Delta S/S_0$ for an unlabeled ternary complex (0.02 $\pm$ 0.02, not shown). For S3P dephasing, ^{15}N-labeled and unlabeled ternary complex $^{31}P\{^{15}N\}$ $\Delta S/S_0$ values were small (0.01 $\pm$ 0.01, not shown) and indistinguishable, indicating ^{31}P-^{15}N distances beyond 8 Å.

Proximity of Glp to arginine sidechains

The $^{15}N\{^{31}P\}$ REDOR spectra of a ternary complex of [*uniform*-^{15}N] EPSP synthase-S3P-Glp are shown in Figure 5 (solid lines). The full-echo spectrum has [ζ- and ε-^{15}N]Arg signals (from 21 arginine residues) centered at 49 and 62 ppm, respectively (Figure 5, bottom, solid line). Because S3P ^{31}P is known to be much farther from [ζ-$^{15}N_2$]Arg than Glp ^{31}P (McDowell et al., 1996b), the two arginines close to Glp ^{31}P are largely responsible for the 38–70 ppm REDOR difference (Figure 5, top, solid line). The large ΔS at 50-ppm from the ζ-^{15}N (Figure 5, top, solid line) was expected from $^{31}P\{^{15}N\}$ experiments on [ζ-$^{15}N_2$]Arg-EPSP synthase (McDowell et al., 1996b). The low-intensity, 62-ppm ε-^{15}N ΔS (Figure 5, top, solid line) was difficult to quantify. Nevertheless, assuming a single nearest-neighbor ε-^{15}N spin, we estimate a 4.5 to 5.7 Å distance to the Glp ^{31}P. The modeling restraint of 5.6 Å (Table 1) was the result of using the BACDOY arginine template (see Methods).

Serine in the binding site

The 100 and 103-ppm resonances in the $^{15}N\{^{31}P\}$ REDOR difference spectrum of [^{15}N]Gly-EPSP

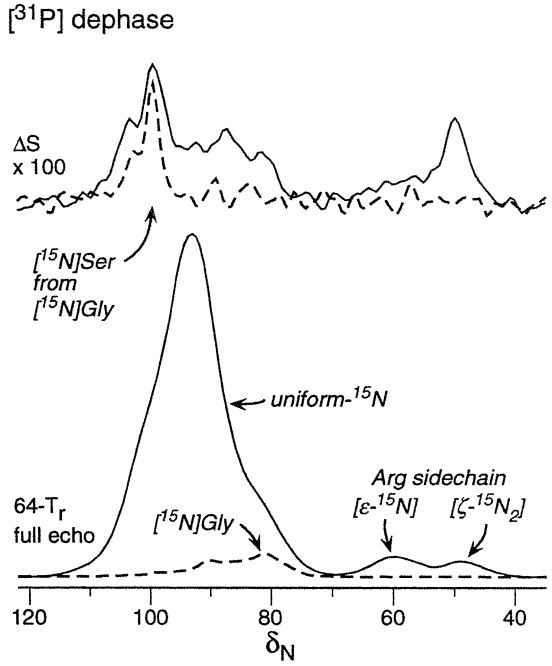

Figure 5. $^{15}N\{^{31}P\}$ REDOR spectra of [*uniform*-^{15}N]EPSP synthase-S3P-[1-^{13}C]Glp (solid lines, 56,716 scans) and [1-^{13}C]Ala-[^{15}N]Gly-EPSP synthase-S3P-Glp (dotted lines, 70,800 scans) lyophilized ternary complexes. The full-echo spectra are shown at the bottom of the figure and the REDOR differences at the top. Spectra for the two samples have been scaled by number of scans and backbone CP transfer and decay rates to allow direct comparison of intensities. The ^{13}C labels were not used in these experiments. The REDOR evolution time was 12.8 ms; MAS speed was 5 kHz.

synthase-S3P-Glp (Figure 3, top, dashed line) are assigned to [^{15}N]Ser, based on chemical shifts (Wishart et al., 1991) and metabolic connectivity to glycine (Waugh, 1996). Normally, ^{15}N resonances in serine occur near 90 ppm (Jacob et al., 1987). However, downfield shifts for ^{15}N near either S3P phosphate or Glp phosphonate have been observed (McDowell et al., 1996b). The same two peaks appear in the $^{15}N\{^{31}P\}$ difference spectrum of [*uniform*-^{15}N]EPSP synthase-S3P-Glp (Figure 5, top, solid line). Some of the [^{15}N]Ser produced from [^{15}N]Gly may have been metabolically processed to [^{15}N]Cys (Waugh, 1996). However, there are only six Cys residues in EPSP synthase, compared to 22 Ser and 37 Gly (Kim et al., 1996). Thus, [^{15}N]Cys was considered unlikely to contribute significant ^{15}N intensity to the REDOR spectra of Figure 5.

In addition to the peptide nitrogens of the one or two serines mentioned above, a few other peptide nitrogens are close to either S3P or Glp ^{31}P (Figure 5, top, solid line). The 81-ppm peak in the $^{15}N\{^{31}P\}$ difference spectrum of [*uniform*-^{15}N] EPSP synthase-S3P-Glp (Figure 5, top, solid line) is assigned to [^{15}N]Gly. This assignment is based on the characteristic glycine chemical shift, and is consistent with the observation that G96A mutation provided Glp resistance to EPSP synthase (Padgette et al., 1991). The absence of an intense 81-ppm peak in the REDOR difference spectrum of [^{15}N]Gly-EPSP synthase-S3P-Glp (Figure 5, top, dashed line), may simply be due to the low incorporation of label for glycine residues (see below) and specific relaxation behavior.

The REDOR full echo spectra (Figure 5, bottom) and cross-polarization (CP) echo spectra for unlabeled ternary complex and [^{15}N]Gly EPSP synthase ternary complex (not shown) were used to estimate the combined average [^{15}N]Ser and [^{15}N]Gly label incorporation levels as 30 $\pm$ 10%. By composition, we would expect an [^{15}N]Gly:[^{15}N]Ser intensity ratio of 1.7. But the observed ratio is only 1.4 (Figure 5, bottom, dashed line), implying lower incorporation of [^{15}N]Gly than [^{15}N]Ser. No attempt was made at a distance determination from this data because of the large uncertainty in S_0 intensity.

REDOR restrained model of the ternary complex of EPSP synthase

Molecular modeling of the binding site of EPSP synthase occupied by S3P and Glp started with the xray coordinates of the unliganded protein (Stallings et al., 1991). For the ligand-protein distances, only the assignments associated with Trp172, Trp337, and His385 were known with certainty. For example, it was known at the start of the modeling that there were two lysines proximate to the ^{31}P of Glp, but not which two of Lys22, Lys340, and Lys411. Different assignments were tried until a model that gave acceptable fits to all the Lys-Glp, Lys-S3P, Arg-Glp, and Arg-S3P dephasing results was found. Molecular dynamics simulations (with energy minimization) were ultimately restrained simultaneously by the 33 distances listed in Table 1. The resulting model is referred to as the REDOR restrained model of the ternary complex, or the REDOR model (PDB code 1Q0I). Backbone atom alignment allowed comparison of the overall folding of the REDOR model (Figure 6, green) with 1G6S (Schönbrunn et al., 2001, Figure 6, yellow). A stereo view of the binding site residues in the REDOR model (Figure 7, colored atoms) is superim-

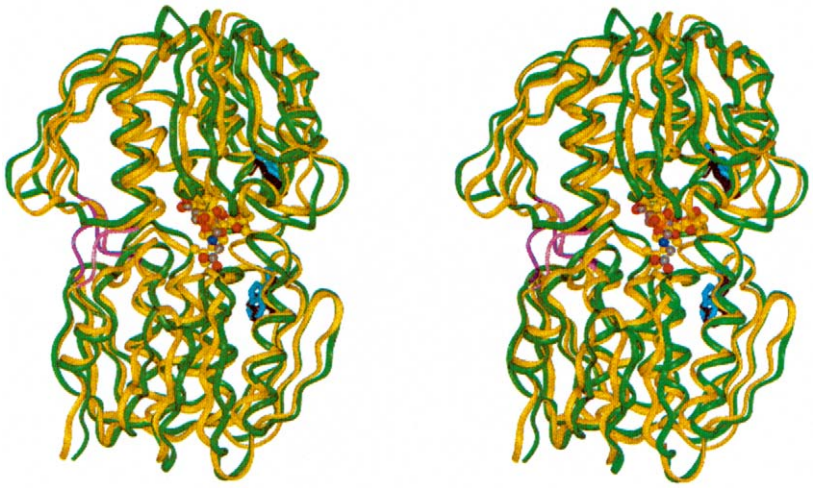

Figure 6. Stereo view of the REDOR model of EPSP synthase-S3P-Glp (green ribbon, purple hinge, black Trp337 and Trp172, atom-colored ligands) overlaid by backbone alignment on 1G6S (yellow ribbon, pink hinge, blue Trp337 and Phe172, yellow ligands).

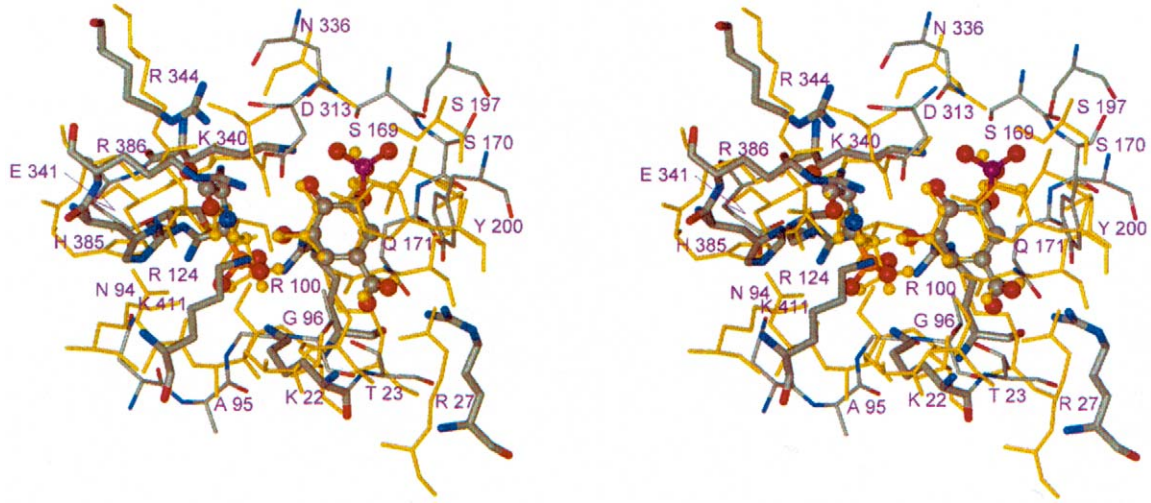

Figure 7. Stereo view of the binding site residues of EPSP synthase-S3P-GlP in the REDOR model (colored atoms) overlaid on 1G6S (yellow). The S3P of the REDOR model was superimposed on the S3P of 1G6S. The comparisons in Figures 9 and 10 use the same alignment.

posed on 1G6S (Figure 7, yellow) by overlaying the S3P molecules.

The REDOR model was created in two phases: global folding and iterative refinement (see Methods). For the global-folding phase of modeling, the distances from ^{19}F labels on the Trp residues (black sticks, Figure 6) to ^{31}P of Glp and S3P provided key long-range distance restraints (Studelska et al., 1996). Adjustments of torsion angles in the "hinge" region (Figure 6, purple) brought the two domains of the protein into proximity.

During the iterative-refinement phase of modeling, the intra- and inter-ligand atom assignments were known at the start, but the REDOR distances depended on accounting for the natural-abundance ^{13}C contributions to dephasing. In our previous work, this accounting was done using a model lattice to specify the positions of the 64 nearest-neighbor carbons (McDowell et al., 1996a). In the present work, the lattice-dependent distances were only used in the global-folding phase of modeling. Then, the lattice was replaced by the protein itself and an iterative process was begun: (i) Carbon positions of the model were used to calculate REDOR dephasing; (ii) calculated and experimental dephasing were compared; (iii) distance restraints were adjusted and their ranges

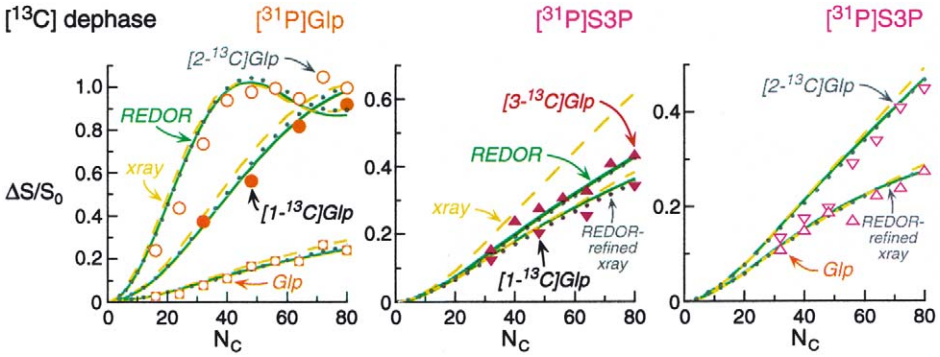

Figure 8. $^{31}P\{^{13}C\}$ REDOR dephasing ($\Delta S/S_0$) for EPSP synthase-S3P-Glp lyophilized ternary complexes as a function of dipolar evolution time with 5 kHz MAS. The Glp in the complexes was either specifically ^{13}C-labeled or natural abundance, as indicated by the italicized notes in the figure. Experimental dephasing (McDowell et al., 1996a) is given by the symbols, which are color-coded to the structures shown in Figures 9 and 10. The solid green, dashed yellow, and dotted gray lines show the calculated dephasing using coordinates from the REDOR model, 1G6S, and the REDOR-refined structure, respectively.

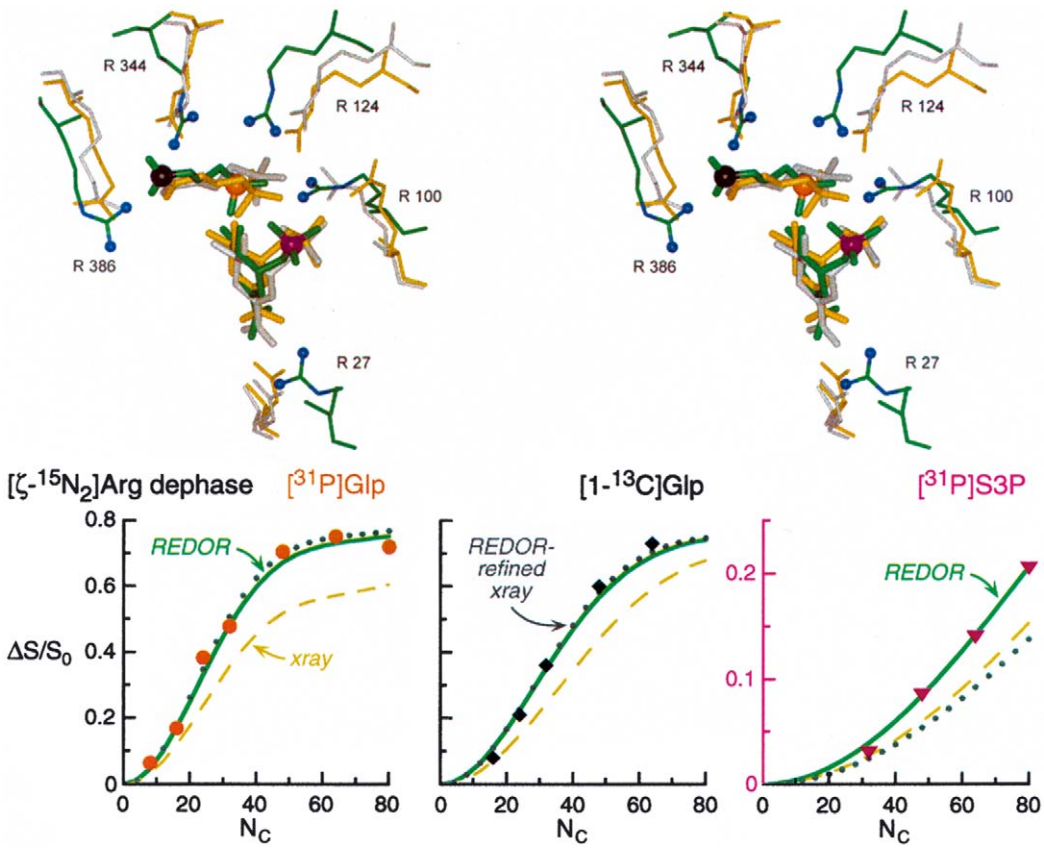

Figure 9. $^{31}P\{^{15}N\}$ (left and right panels) and $^{13}C\{^{15}N\}$ (center panel) REDOR dephasing ($\Delta S/S_0$) for [ζ-$^{15}N_2$]Arg-EPSP synthase-S3P-[1-^{13}C]Glp lyophilized ternary complex as a function of dipolar evolution time. Experimental dephasing is given by the symbols, which are color-coded to the structure shown at the top of the figure in stereo. The dephasing nuclei of the arginine sidechains are small blue spheres in the REDOR model, which is overlaid by alignment of S3P on 1G6S (yellow), and on the REDOR refinement of 1G6S (gray). The solid green, dashed yellow, and dotted gray lines show the calculated dephasing using coordinates from the REDOR model, 1G6S, and the REDOR-refined structure, respectively. Only the 64 rotor cycle data were published previously (McDowell et al., 1996b).

reduced; (iv) molecular dynamics and energy minimization were performed. As the model was refined, the carbon positions changed slightly. These changes affected the calculated natural-abundance dephasing, which, in turn, altered the ^{31}P-^{13}C distances used as restraints and resulted in the adjustments of step (iii). A few iterations resulted in reasonable fits to all of the intra- and inter-ligand ^{31}P{^{13}C} REDOR data (Figure 8, symbols). The calculations included the positions of all carbons (approximately 100) within 10 Å of either S3P or Glp ^{31}P. Calculations using a 12-Å radius had only a 1% change in $\Delta S/S_0$ and a substantially lengthened calculation time. For the REDOR model of Figures 6 and 7, 101 carbon positions gave rise to 5000 possible configurations having 0, 1, or 2 natural-abundance ^{13}C's in addition to a specific ^{13}C label. REDOR dephasing ($\Delta S/S_0$) was calculated for each of these configurations, appropriately weighted, and then summed (Figure 8, green lines).

Although REDOR results indicated at least one or two [^{15}N]Ser residues near ^{31}P in the binding site of the ternary complex (Figure 5), their identities and assignments (to the ^{31}P of S3P, or Glp, or both) could not be determined from the NMR results. Because it was conceivable that rearrangement occurred when Glp was present (Quiocho, 1990; Shuttleworth et al., 1994; Gehring et al., 1998, Krekel et al., 1999), we chose not to use the serine restraints to S3P reported for either xray structure of the EPSP synthase-S3P binary complex (2.4-Å resolution, Franz et al., 1997; 1G6T, Schönbrunn et al., 2001). The Ser169 N to S3P O distances differ by >1 Å between the Franz et al., structure and 1G6T. Our model has longer, but reasonable, distances than any of the crystal structures, despite our not using any restraints. Furthermore, Ser169 O to S3P O distances differ between 1G6T (binary complex) and 1G6S (ternary complex). This further supports structural changes to the enzyme on Glp binding. Similarly, because no NMR data on the ternary complex confirmed the S3P-Tyr200 interactions found in the binary complex (Franz et al., 1997), they were not included in the modeling.

The arginine sidechain to Glp distances in the global-folding phase of the modeling came from small-molecule templates (see Methods). The difference between using two arginines to select starting templates and four arginines was small, but not negligible. Consequently, a few iterations of distance and restraint adjustments (similar to those described above) were needed to obtain a good fit between the REDOR dephasing data (Figure 9, bottom, symbols) and calculations based on the REDOR model (Figure 9, bottom, green lines). A simplified stereo view of the REDOR model binding site arginines (carbon, green; nitrogen, blue) and ligands is also shown (Figure 9, top). The S3P and Glp atoms rendered as balls are color-coded to match the dephasing plot symbols (Figure 9, bottom). The four closest arginines (eight ζ-^{15}N labels, Figure 9, top, blue balls) were used to calculate the ^{31}P{^{15}N} and ^{13}C{^{15}N} dephasing (Figure 9, bottom, green lines). Arg27 was among the four closest only for S3P ^{31}P. The Arg27 to S3P carboxyl distances reported for the binary complex (Franz et al., 1997) were consistent with the REDOR data (Figure 4) and were used as restraints for modeling (Table 1). In the REDOR model, all four distances between Glp ^{31}P and ζ-^{15}N of Arg100 and Arg124 (Table 1) are consistent with hydrogen-bonding interactions between the phosphate and guanidino groups. Arg344 and Arg386 each have one ζ-^{15}N distance consistent with hydrogen bonding to the Glp carbonyl. (See ^{13}C-^{15}N distances, Table 1). The REDOR model (Figure 9, bottom, green lines) is an excellent match to the REDOR data (Figure 9, bottom, symbols). Changing the P-Nζ arginine distances by ± 0.2 Å made a noticeably poorer fit; this indicates that the restraints used in the modeling (Table 1) are accurate.

The experimental dephasing from REDOR experiments on [ε-^{15}N]Lys-EPSP synthase-S3P-[1-^{13}C]Glp synthase dephasing (Figure 10, symbols) is consistent with the predictions of the REDOR model (green lines). Calculated multi-spin effects were small for the three [ε-^{15}N]Lys interactions with Glp and S3P. The minor adjustments of the published distances (McDowell et al., 1996b) needed to optimize the model were within the error of the measurements. The locations of the three lysine ε-^{15}N (Figure 10, blue balls) in the REDOR model of the EPSP synthase binding site are shown at the top of the figure, along with that of the [1-^{13}C]Glp carbon label, (black ball), Glp ^{31}P (orange ball), and S3P ^{31}P (pink ball).

REDOR model and the X-ray structure

With only two long-range restraints to close the two domains of the REDOR model (Figure 6, green), the good overall agreement with the 1G6S structure (Schönbrunn et al., 2001, Figure 6, yellow) was somewhat surprising, given that even a crystal can exhibit a variety of relative domain structures (Larsen et al., 1997). In Figure 6, made by alignment of the backbone atoms, the S3P and Glp molecules in the two structures

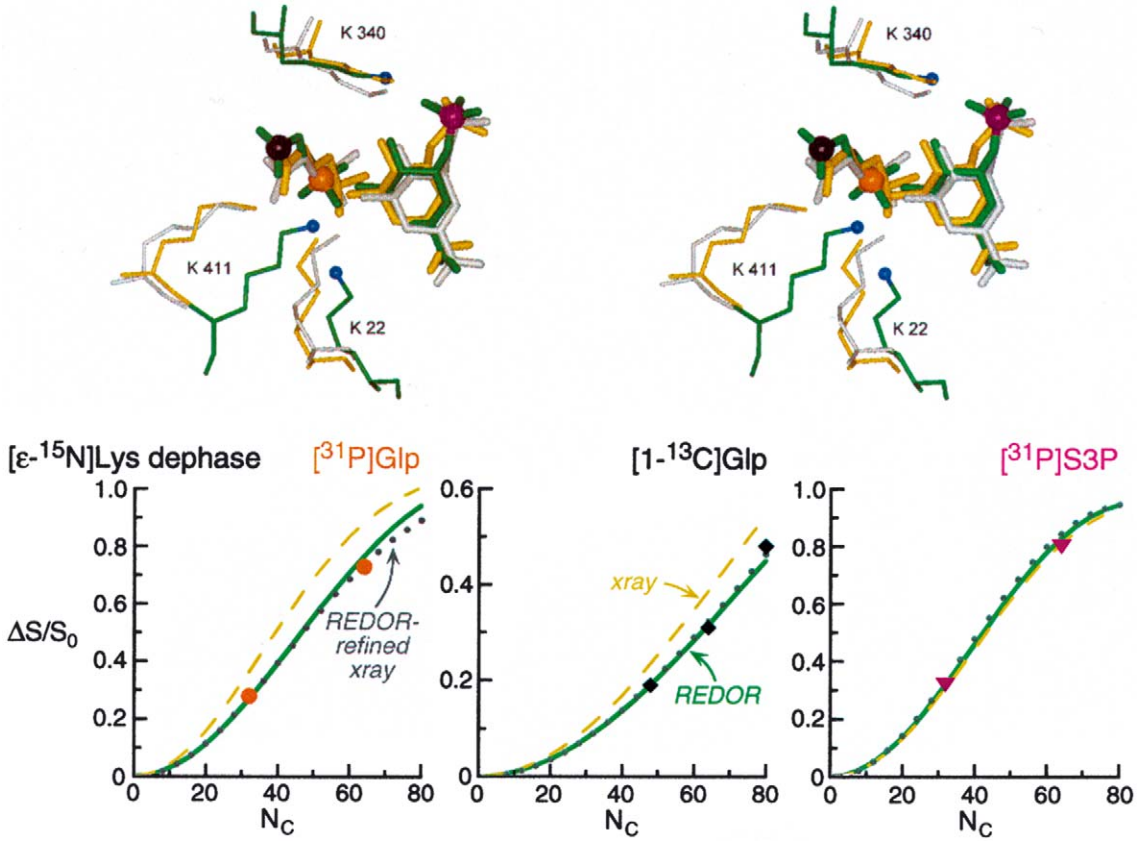

Figure 10. $^{31}P\{^{15}N\}$ (left and right panels) and $^{13}C\{^{15}N\}$ (center panel) REDOR dephasing ($\Delta S/S_0$) for [ε-^{15}N]Lys-EPSP synthase-S3P-[1-^{13}C]Glp lyophilized ternary complex as a function of dipolar evolution time. Experimental dephasing (McDowell et al., 1996b) is given by the symbols, which are color-coded to the structure shown at the top of the figure in stereo. The dephasing nuclei of the lysine sidechains are small blue spheres in the REDOR model, which is overlaid by alignment of S3P on 1G6S (yellow), and on the REDOR refinement of 1G6S (gray). The solid green, dashed yellow, and dotted gray lines show the calculated dephasing using coordinates from the REDOR model, 1G6S, and the REDOR-refined structure, respectively.

are slightly offset from each other. By overlaying the S3P molecules, we compared all binding-site residues (Figure 7, REDOR model – colored atoms, 1G6S – yellow), arginine residues (Figure 9), and lysine residues (Figure 10). Differing sidechain positions between 1G6S and the REDOR model were expected for residues having no REDOR restraints such as Ser169 and Tyr200 (Figure 7), but not for arginine (Figure 9) and lysine (Figure 10) sidechains having REDOR restraints. The 1G6S calculations match two of the three His385 REDOR results reasonably well (Table 1).

Multi-spin REDOR dephasing was calculated using the 1G6S coordinates (yellow dashed lines, Figures 8–10). Except for the [3-^{13}C]Glp complex, the $^{31}P\{^{13}C\}$ REDOR data were well fit by predictions based on the coordinates of 1G6S (Figure 8). However, none of the [ζ-$^{15}N_2$]Arg-EPSP synthase REDOR results matched the predictions based on 1G6S coordinates (Figure 9, bottom). The agreement between 1G6S calculations and the [ε-^{15}N]Lys-EPSP synthase REDOR results was good for S3P $^{31}P\{^{15}N\}$ data (Figure 10, right panel), but only moderately good for the Glp ^{31}P or ^{13}C observe data (left and center panels).

With the exceptions of Arg27 and Arg124, there are significant quantitative differences in arginine sidechain distances to S3P and Glp. The largest difference is that Arg100 in 1G6S is too far away from the Glp phosphate to have hydrogen-bonding interactions (Figure 9, top, Table 1). The distance differences (1.2–2.9 Å, Table 1) are well outside the error limits of the REDOR measurement and the uncertainty implied by the temperature factors in 1G6S. This explains the poor fit of 1G6S (Figure 9, yellow dashed lines) to

the Glp P observe data (Figure 9, left, orange circles). The somewhat smaller distance differences found for Arg344 and Arg386 interacting with Glp carbonyl (0.6–1.9 Å, Table 1) are noticeable both in the stereo view (Figure 9, top), and in the ^{13}C–ζ-^{15}N 1G6S calculated REDOR curve (Figure 9, bottom, center, yellow dashed line). This curve fits the data (black diamonds) better than might be expected because the one ζ-^{15}N of Arg344 that is too close partially compensates for Arg386 being too far away.

The REDOR model and 1G6S have similar distances between S3P, Glp, and lysines (Table 1). The S3P phosphate - Lys340 orientations match in the two structures (Figure 10, top), as do their dephasing curves (Figure 10, bottom right). For Glp interactions with lysines, the differences between distances in 1G6S and the REDOR model (0.1–0.4 Å, Table 1) are within experimental error. However, the sum of three small distance changes yields a somewhat poorer fit for the 1G6S calculated REDOR curves (Figure 10, bottom, yellow dashes, left and center) than for the REDOR model (Figure 10, green lines). The large differences in geometry of the lysine residues near Glp (Figure 10, top) arise from different assignments in the REDOR model compared to 1G6S (see Table 1). While the literature clearly identified which lysines were in the binding site (see Introduction), the assignments were ambiguous. The TEDOR-REDOR data (McDowell et al., 1996b) suggested that :
(1) the one lysine interacting with S3P phosphorous was distant from the Glp carboxyl; and,
(2) only one (of the two lysines close to Glp P) was 'shared' with the carboxyl-end of Glp.
For the model reported here, we chose Lys411 as being 'shared' (Table 1). By contrast, in 1G6S, Lys22 is 'shared'. In both structures, only one lysine is within 4.5 Å of the Glp carboxyl. The 5.6 Å [1-^{13}C]Glp to [ε-^{15}N]Lys411 distance in 1G6S was not found by TEDOR-REDOR because conditions were chosen to detect distances < 4.5 Å (McDowell et al., 1996b). While we succeeded in our goal to create a model that fits all the NMR data, we never assumed this model was unique. Indeed, it is not. The next section describes a model derived from 1G6S that is also a reasonable fit to the NMR data.

REDOR refinement of the xray structure

Essentially the same restraints used to create the REDOR model were applied using the 1G6S structure as the source of the starting coordinates (Table 1). Relatively small changes in lysine sidechain positions (Figure 10, gray) were sufficient for this REDOR-refined structure (PDB code 1Q0J) to satisfy the ^{31}P{^{15}N} and ^{13}C{^{15}N} dephasing for [ε-^{15}N]Lys-EPSP synthase-S3P-[1-^{13}C]Glp (Figure 10, dotted lines) and inter-ligand restraints (Table 1). However, a substantial change in Arg100 location was necessary (Figure 9, top, gray) to satisfy the REDOR data. Smaller adjustments were adequate for the other arginines. In general, the calculated multi-spin REDOR dephasing for the REDOR-refined structure (Figure 9, bottom, gray dotted lines) fit the data for [ζ-^{15}N$_2$]Arg-EPSP synthase-S3P-[1-^{13}C]Glp as well as the REDOR model. There was no obvious way to correct the one poor fit by restraint adjustment (Figure 9, right panel). The REDOR-refined structure fit all the histidine REDOR results moderately well (Table 1).

Discussion

The positions of the basic sidechains of the five arginines, three lysines, and histidine in the binding site of EPSP synthase are crucial in determining the binding of the negatively charged S3P and Glp ligands. Although there is agreement between the REDOR model and the xray crystal structure as to the identity of these nine residues, there are substantive differences in their locations. Of these, the most significant differences are in the arginine sidechain interactions. For arginines, the differences between REDOR and xray determined positions are real. The errors in the REDOR distances (see footnotes to Table 1), and the uncertainties in xray positions (associated with the Debye–Waller factors for the arginines in the binding site), are both small.

The most likely reason for the disagreement between the arginine results in the REDOR model and 1G6S is that different sample preparation methods were employed. A protein crystal suitable for diffraction experiments is necessarily ordered on both short and long distance scales. Crystallization conditions can influence protein and ligand conformations (a few examples: Kurinov and Harrison, 1995; Huang et al., 1996; Renatus et al., 1998; Berisio et al.; 1999; Stubbs et al., 2002). A lyophilized protein powder suitable for solid-state NMR experiments is less ordered than a crystal, but it is not disordered. Relatively narrow phosphorous lines and phosphorous chemical shifts that match those found by solution NMR (Christensen and Schaefer, 1993; McDowell et al., 1996a, b;

Studelska et al., 1996) indicate that the lyophilized sample preserves the solution structure of the ternary complex binding site. (Phosphorous chemical shifts are quite sensitive to their local environment.)

The 1–3 Å differences between the arginine positions of the REDOR model and REDOR-refined xray structure versus 1G6S (Table 1) could be important for enzyme function. In drug design, differences of this magnitude would imply addition (or removal) of 1 or 2 carbon atoms to optimize a template (Marc Adler, Berlex Biosciences, personal communication). We are not alone in believing that these small changes can be important. A group of crystallographers found 'small but significant structural changes which provide clues to the function of a biological macromolecule' (Berisio et al., 1999), by changing the pH at which crystals were grown. The REDOR model of Figures 5 and 6, and the REDOR-refined xray structure (Figures 9 and 10, Table 1) are both consistent with the solid-state NMR data. Just as solution NMR structures sometimes differ from xray structures (2 examples: Hodsdon and Cistola, 1997; Lukin et al., 2003), our lyophilized solution, i.e., solid-state, NMR structures can differ from xray structures. We believe that some distances to the residues surrounding S3P and Glp in the binding site of EPSP synthase *in solution* differ from those determined by xray analysis.

Although the data collection and analysis of Table 1 took many samples and many experiments to complete, and can hardly be considered a high-throughput operation, the insightful detail of the REDOR model demonstrates the capabilities of solid-state NMR in general, and REDOR in particular, as tools for structural biology. If the liganded protein does not crystallize because of relatively weak binding or conformational mobility, REDOR offers the opportunity to gain atomic-level resolution for the binding site without a crystal. The use of REDOR to refine or enhance an existing crystal structure (as illustrated in Figures 9 and 10), or a calculated structure (derived from homology or *ab initio* modeling), is appealing in its simplicity. In this sort of application, a few complementary labels in ligands and proteins will immediately provide a test of the validity of the proposed structure (Wang et al., 1997).

Acknowledgements

The authors are grateful to William Stallings, Monsanto Company, St. Louis, MO, for providing a full set of coordinates from the crystal structure of unliganded EPSP synthase in 1994. Allyson Christensen was responsible for the growth of [^{15}N]Gly-EPSP synthase. This work was supported by NIH grant EB-01964.

References

Altschul, S.F., Gish, W., Miller, W., Myers, E.W. and Lipman, D.J. (1990) *J. Mol. Biol.*, **215**, 403–410.

Anderson, K.S. and Johnson, K.A. (1990) *Chem. Rev.*, **90**, 1131–1149.

Anderson, K.S., Sikorski, J.A. and Johnson, K.A. (1988) *Biochemistry*, **27**, 1604–1610.

Berisio, R., Lamzin, V.S., Sica, F., Wilson, K.S., Zagari, A. and Mazzarella, L. (1999) *J. Mol. Biol.*, **292**, 845–854.

Berman, H.M., Westbrook, J., Feng, Z., Gilliland, G., Bhat, T.N., Weissig, H., Shindyalov, I.N. and Bourne, P.E. (2000) *Nucl. Acids Res.*, **28**, 235–242.

Beusen, D.D., McDowell, L.M., Slomczynska, U. and Schaefer, J. (1995) *J. Med. Chem.*, **38**, 2742–2747.

Castellino, S., Leo, G.C., Sammons, R.D. and Sikorski, J.A. (1991) *J. Org. Chem.*, **56**, 5176–5181.

Chan, J.C.C. and Eckert, H. (2000) *J. Magn. Reson.*, **147**, 170–178.

Christensen, A.M. and Schaefer, J. (1993) *Biochemistry*, **32**, 2868–2873.

Duncan, K., Lewendon, A. and Coggins, J.R. (1984) *FEBS Lett.*, **170**, 59–63.

Franz, J.E., Mao, M.K. and Sikorski, J.A. (1997) *Glyphosate: A Unique Global Herbicide*, American Chemical Society, Washington, DC.

Gehring, K., Zhang, X., Hall, J., Nikaido, H. and Wemmer, D.E. (1998) *Biochem. Cell Biol.*, **76**, 189–197.

Goetz, J.M. and Schaefer, J. (1997) *J. Magn. Reson.*, **127**, 147–154.

Gullion, T. and Schaefer, J. (1989a) *J. Magn. Reson.*, **81**, 196–200.

Gullion, T. and Schaefer, J. (1989b) *Adv. Magn. Reson.*, **13**, 57–83.

Gullion, T. and Schaefer, J. (1991) *J. Magn. Reson.*, **92**, 439–442.

Gullion, T. and Vega, S. (1992) *Chem. Phys. Lett.*, **194**, 423–428.

Gullion, T., Baker, D.B. and Conradi, M.S. (1990) *J. Magn. Reson.*, **89**, 479–484.

Hing, A.W., Tjandra, N., Cottam, P.F., Schaefer, J. and Ho, C. (1994) *Biochemistry*, **33**, 8651–8661.

Hodsdon, M.E. and Cistola, D.P. (1997) *Biochemistry*, **36**, 2278–2290.

Huang, D.B., Ainsworth, C.F., Stevens, F.J. and Schiffer, M. (1996) *Proc. Natl. Acad. Sci. U.S.A.*, **93**, 7017–7021.

Huynh, Q.K. (1990) *J. Biol. Chem.*, **265**, 6700–6704.

Huynh, Q.K. (1991) *Arch. Biochem. Biophys.*, **284**, 407–412.

Huynh, Q.K. (1992) *Biochem. Biophys. Res. Commun.*, **185**, 317–322.

Huynh, Q.K. (1993) *Biochem. J.*, **290**, 525–530.

Huynh, Q.K., Kishore, G.M. and Bild, G.S. (1988a) *J. Biol. Chem.*, **263**, 735–739.

Huynh, Q.K., Bauer, S.C., Bild, G.S., Kishore, G.M. and Borgmeyer, J.R. (1988b) *J. Biol. Chem.*, **263**, 11636–11639.

Jacob, G.S., Schaefer, J., Garbow, J.R. and Stejskal, E.O. (1987) *J. Biol. Chem.*, **262**, 254–259.

Kim, D.H., Tucker-Kellogg, G.W., Lees, W.J. and Walsh, C.T. (1996) *Biochemistry*, **35**, 5435–5440.

Knowles, P.F. and Sprinson, D.B. (1970) *Meth. Enzymol.*, **17A**, 351–352.

Krekel, F., Oecking, C., Amrhein, N. and Macheroux, P. (1999) *Biochemistry*, **38**, 8864–8878.

Kurinov, I.V. and Harrison, R.W. (1995) *Acta Cryst. D Biol. Cryst.*, **D51**, 98–109.

Larsen, T.M., Benning, M.M., Wesenberg, G.E., Rayment, I. and Reed, G.H. (1997) *Arch. Biochem. Biophys.*, **345**, 199–206.

Leo, G.C., Castellino, S., Sammons, R.D. and Sikorski, J.A. (1992) *Bioorg. Med. Chem. Lett.*, **2**, 151–154.

Lukin, J.A, Kontaxis, G., Simplaceanu, V., Yuan, Y., Bax, A. and Ho, C. (2003) *Proc. Natl. Acad. Sci. U.S.A.*, **100**, 517–520.

Marshall, G.R., Beusen, D.D., Kociolek, K., Redlinski, A.S., Leplawy, M.T., Pan, Y. and Schaefer, J. (1990) *J. Am. Chem. Soc.*, **112**, 963–966.

McDowell, L.M., Klug, C.A., Beusen, D.D. and Schaefer, J. (1996a) *Biochemistry*, **35**, 5395–5403.

McDowell, L.M., Schmidt, A., Cohen, E.R., Studelska, D.R. and Schaefer, J. (1996b) *J. Mol. Biol.*, **256**, 160–171.

Mehta, A.K., Hirsh, D.J., Oyler, N., Drobny, G.P. and Schaefer, J. (2000) *J. Magn. Reson.*, **145**, 156–158.

Millican, R.C. (1970) *Meth. Enzymol.*, **17A**, 352–354.

Mousedale, D.M. and Coggins, J.R. (1995) *Planta*, **163**, 241–249.

O'Connor, R.D. and Schaefer, J. (2002) *J. Magn. Reson.*, **154**, 46–52.

Olins, P.O., Devine, C.S., Rangwala, S.H. and Kavka, K.S. (1988) *Gene*, **73**, 227–235.

Padgette, S.R., Re, D.B., Gasser, C.S., Eichholtz, D.A., Frazier, R.B., Hironaka, C.M., Levine, E.B., Shah, D.M., Fraley, R.T. and Kishore, G.M. (1991) *J. Biol. Chem.*, **266**, 22364–22369.

Padgette, S.R., Smith, C.E., Huynh, Q.K. and Kishore, G.M. (1988) *Arch. Biochem. Biophys.*, **266**, 254–262.

Pan, Y., Gullion, T. and Schaefer, J. (1990) *J. Magn. Reson.*, **90**, 330–340.

Quiocho, F.A. (1990) *Phil. Trans. Royal Soc. London. Ser. B Biol. Sci.*, **326**, 341–351; Discussion 351–352.

Raleigh, D.P., Levitt, M.H. and Griffin, R.G. (1988) *Chem. Phys. Lett.*, **146**, 71–76.

Renatus, M., Bode, W., Huber, R., Sturzebecher, J. and Stubbs, M.T. (1998) *J. Med. Chem.*, **41**, 5445–5456.

Rueppel, M.L., Brightwell, B.B., Schaefer, J. and Marvel, J.T. (1977) *J. Agric. Food Chem.*, **25**, 517–528.

Schönbrunn, E., Eschenburg, S., Shuttleworth, W.A., Schloss, J.V., Amrhein, N., Evans, J.N.S. and Kabsch, W. (2001) *Proc. Natl. Acad. Sci. USA*, **98**, 1376–1380.

Selvapandiyan, A., Ahmad, S., Majumder, K., Arora, N. and Bhatnagar, R.K. (1996) *Biochem. Mol. Biol. Int.*, **40**, 603–610.

Selvapandiyan, A., Majumder, K., Fattah, F.A., Ahmad, S., Arora, N. and Bhatnagar, R.K. (1995) *FEBS Lett.*, **374**, 253–256.

Shuttleworth, W.A. and Evans, J.N.S. (1994) *Biochemistry*, **33**, 7062–7068.

Shuttleworth, W.A. and Evans, J.N.S. (1996) *Arch. Biochem. Biophys.*, **334**, 37–42.

Shuttleworth, W.A., Pohl, M.E., Helms, G.L., Jakeman, D.L. and Evans, J.N.S. (1999) *Biochemistry*, **38**, 296–302.

Stalker, D.M., Hiatt, W.R. and Comai, L. (1985) *J. Biol. Chem.*, **260**, 4724–4728.

Stallings, W.C., Abdel-Meguid, S.S., Lim, L.W., Shieh, H.-S., Dayringer, H.E., Leimgruber, N.K., Stegeman, R.A., Anderson, K.S., Sikorski, J.A., Padgette, S.R. and Kishore, G.M. (1991) *Proc. Nat. Acad. Sci. USA*, **88**, 5046–5050.

Stauffer, M.E., Young, J.K. and Evans, J.N.S. (2001) *Biochemistry*, **40**, 3951–3957.

Stauffer, M.E., Young, J.K., Helms, G.L. and Evans, J.N.S. (2001) *FEBS Lett.*, **499**, 182–186.

Steinrücken, H.C. and Amrhein, N. (1980) *Biochem. Biophys. Res. Commun.*, **94**, 1207–1212.

Stubbs, M.T., Reyda, S., Dullweber, F., Moller, M., Klebe, G., Dorsch, D., Mederski, W.W.K.R. and Wurziger, H. (2002) *ChemBioChem.*, **3**, 246–249.

Studelska, D.R., Klug, C.A., Beusen, D.D., McDowell, L.M. and Schaefer, J. (1996) *J. Am. Chem. Soc.*, **118**, 5476–5477.

Studelska, D.R., McDowell, L.M., Espe, M.P., Klug, C.A. and Schaefer, J. (1997) *Biochemistry*, **36**, 15555–15560.

Wang, J., Balazs, Y.S. and Thompson, L.K. (1997) *Biochemistry*, **36**, 1699–1703.

Waugh, D.S. (1996) *J. Biomol. NMR*, **8**, 184–192.

Weiss, U. and Mingioli, E.S. (1956) *J. Am. Chem. Soc.*, **78**, 2894–2898.

Weldeghiorghis, T.K. and Schaefer, J. (2003) *J. Magn. Reson.*, in press.

Wishart, D.S., Sykes, B.D. and Richards, F.M. (1991) *J. Mol. Biol.*, **222**, 311–333.

Wu, J., Xiao, C., Yee, A.F., Goetz, J.M. and Schaefer, J. (2000) *Macromolecules*, **33**, 6849–6852.